LA MÉTROLOGIE AU CŒUR DES TECHNOLOGIES CONTEMPORAINES

Proposition de méthodologie de mesure champ proche électrique à faible coût avec un imageur à micro-ondes

First steps of low-cost PCB E-near field radiation metrology with microwave imaging scanner

N. Delille[1], J. Rossignol[1], S. Lalléchère[2], B. Ravelo[3]

[1]Univ. Bourgogne Europe, Dijon, France, {jerome.rossignol@ube.fr, nolane_delille@etu.u-bourgogne.fr}
[2]Safran Tech, Paris-Saclay, France, sebastien.lallechere@safrangroup.com
[3]NUIST, Nanjing 210044, Jiangsu, China, blaise.ravelo@yahoo.fr

Mots clés : champ électrique champ proche (E-NF), compatibilité électromagnétique (CEM), instrumentation, technique d'imagerie micro-ondes
Keywords: Electric near-field (E-NF), PCB emission, radiated electromagnetic compatibility (EMC), microwave imaging technique

Résumé/Abstract

Ce travail porte sur le développement d'un dispositif d'imagerie micro-ondes à bas cout (< 800 €) destiné à la cartographie des champs proches électrique et magnétique émis par des circuits imprimés (PCB). Il s'inscrit dans une démarche de recherche ouverte avec une forte vocation pédagogique. L'imageur repose sur une sonde monopole planaire pour la détection du champ électrique à 5,36 GHz, ainsi qu'une sonde magnétique dédiée. L'ensemble du système s'appuie sur des solutions à bas coût, incluant la fabrication de circuits micro-rubans et un banc de mesure automatisé combinant une imprimante 3D et une radio logicielle (SDR). Une attention particulière est portée à la versatilité du dispositif intégrant l'interface CNC, programmé en Python, et conçu pour être facilement adaptable à divers contextes de mesure grâce aux avancées récentes en impression 3D. Cette modularité avec CNC ouvre la voie à la réalisation d'une série de systèmes reproductibles, en vue de constituer une base de données expérimentale de grande ampleur. Celle-ci pourra être exploitée pour l'entraînement de modèles d'apprentissage profond, avec pour objectif une caractérisation automatique et prédictive des comportements électromagnétiques des circuits.

This work presents the development of a low-cost microwave imaging system (< €800) for mapping electric near-field (E-NF) and magnetic near-field (H-NF) radiated by printed circuit boards (PCBs). The project includes in the frame of an open research initiative with strong educational objectives. The imaging platform is based on a planar monopole probe for electric field detection at 5.36 GHz combined with a dedicated magnetic field probe. The setup relies on cost-effective solutions, including manufactured microstrip circuits and an automated measurement bench integrating a 3D printer operating with computer numerical control (CNC) and a software-defined radio (SDR). Special attention is paid to the versatility of the CNC system, which is fully programmable in Python and designed to be easily reconfigurable for various measurement scenarios, leveraging recent advances in 3D printing technologies. This modular approach enables the development of a series of reproducible systems aimed at building a large-scale experimental database. Such a dataset can be used to train deep learning models, paving the way for automated and predictive electromagnetic compatibility (EMC) characterization of electronic circuits.

1 Introduction

Nowadays, despite the spectacular technological development progress towards the 6G communication system, the electromagnetic compatibility (EMC) constraint remains an open challenge due to the tremendous increase of electronic printed circuit board (PCB) design density [1-2]. To deal with EMC issues, the electromagnetic (EM) radiation measurement of whether electric or magnetic in the near-field (NF) region is a well-established technique for monitoring defects in electronic circuits. When the PCB operates in a confined space, the NF emission becomes a breakthrough for EMC engineers [3]. The EM NF scanning technique is particularly useful to solve electrical and electronic system problems as the EMC source localization [4-5]. The NF emission scanners must follow EM emission measurement technique standard as IEC-61967 [6]. For example, the radiated emission illustrated by the synoptic diagram shown in Figure 1 must be validated with the 50-Ω microstrip line PCB as device under test (DUT) [7].

One of metrological challenges expected in radiated EMC engineering, the NF measurement performance depends on the probe characteristics [8]. Several ambitious developments of EMC radiated NF test benches were designed and tested in the literature [3-5, 7, 9-10].

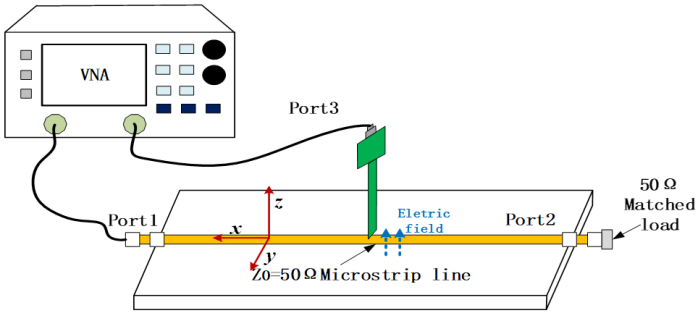

Figure 1: E-NF probe test synoptic diagram [7]

Some NF probes were alongside commercially available imaging systems [11]. These design solutions rely typically on high-precision positioning systems, ultra-sensitive electric (E)-field probes, and laboratory-grade high-frequency spectrum analyzers. Most PCB EM radiation scanning techniques are based on the magnetic (H)-field probe [12-13]. Such systems, designed for research or industrial qualification, come with development or acquisition costs which may reach tens of thousands of euros per complete setup [11]. While they offer high-resolution and highly accurate field mapping, their operation requires advanced expertise, involves complex calibration procedures, and renders them impractical for educational use both in terms of cost and usability. However, the emergence of 5G communications has ushered in an era of more affordable high-frequency measurement tools, particularly using software-defined radios (SDRs). This trend opens the way to the democratization of NF measurements at microwave frequencies by addressing the economic accessibility criteria necessary to equip students with enough imagers for hands-on lab sessions. To meet this need, a target unit cost of €800 per imager is considered acceptable for widespread deployment, assuming a relative positioning accuracy (depending on the positioning model used). The electromagnetic interference (EMI) imaging system must be intuitive and easy to use for undergraduate students [14], while being robust and reliable enough to withstand intensive use and occasional mishandling during laboratory activities. Finally, in the context of a long-term project aimed at integrating artificial intelligence (AI) models into EMC applications, the number of available imaging units becomes a critical factor. The AI-based approaches require large datasets for training, making it essential to maximize the number of imagers in operation to collect sufficient measurement data. The approach presented in this article fully aligns with the goal of democratizing low-cost EMC measurement tools. The result of a long-standing collaboration between the authors, this work provides a detailed overview of the developed samples and probes fabricated with computer numerical control (CNC) milling, as well as the experimental setup used for measurements. The E-NF test bench validation results will also be discussed, offering insights into the system's performance for the intended applications.

2 Design and fabrication of radiating PCB DUT and NF probes

Figure 2: CNC milling used, spatial resolution, electric and magnetic probes

The design and implementation of PCB DUT and NF probes under study belongs in the frame of pedagogical unit in the electronics and electrical engineering major in the University of Bourgogne Europe. All E- and H-NF probes including the test samples are manufactured by CNC milling (Figure 2-❶: here using a Technodrill 3D CIF). Figure 2 depicts the apparatus, the minimum spatial resolution (Figure 2-❷) achievable on the circuit, and the probes obtained. The E-NF probe is based on a coplanar design (Figure 2-❸) with an ungrounded tip; its length was chosen to meet narrow-band measurement requirements at 5.3 GHz. The tip width is limited by the mechanical resolution of the CNC and is typically on the order of tens of micrometers. In first approximation, the E-probe orientation can be associated to the NF field tangential component.

The E-NF probe represented by a microstrip monopole antenna printed on Rogers substrate with 0.3 mm thickness and relative permittivity ε_r=8 photographed in Figure 3 was designed, fabricated and tested for the imager test bench. This probe has a challenging performance in terms of operation frequency f_0 and the cylindrical antenna diameter of about 0.05 mm. The probe arm length enables it to adapt to the targeted scanning frequency. Table 1 indicates the E-NF probe specifications as f_0, quality factor Q, reflection coefficient $S_{11}(f_0)$ and -10 dB cut-off frequencies, lower f_{low} and upper f_{up} ones.

Table 1: Designed E-NF probe specifications

Designation	f_0	$S_{11}(f_0)$	Q	f_{low}	f_{up}
Value	5.36 GHz	-24.79 dB	44.6	5.3 GHz	5.42 GHz

The second type is a H-field probe (Figure 2-❹), inspired by the design presented in [15]. It consists of a grounded coplanar line followed by a circular loop, where the final third of the loop devoid of ground plane is the actual active sensing region. This simple design for both probes could be used on a basis for a lab on double layer PCB manufacturing using the tools available at the lab like the Technodrill. The microstrip samples layout are also presented (Figures 3), incorporating common defects such as cut (open) lines, faulty segments, 90° bends, and rounded or chamfered corners.

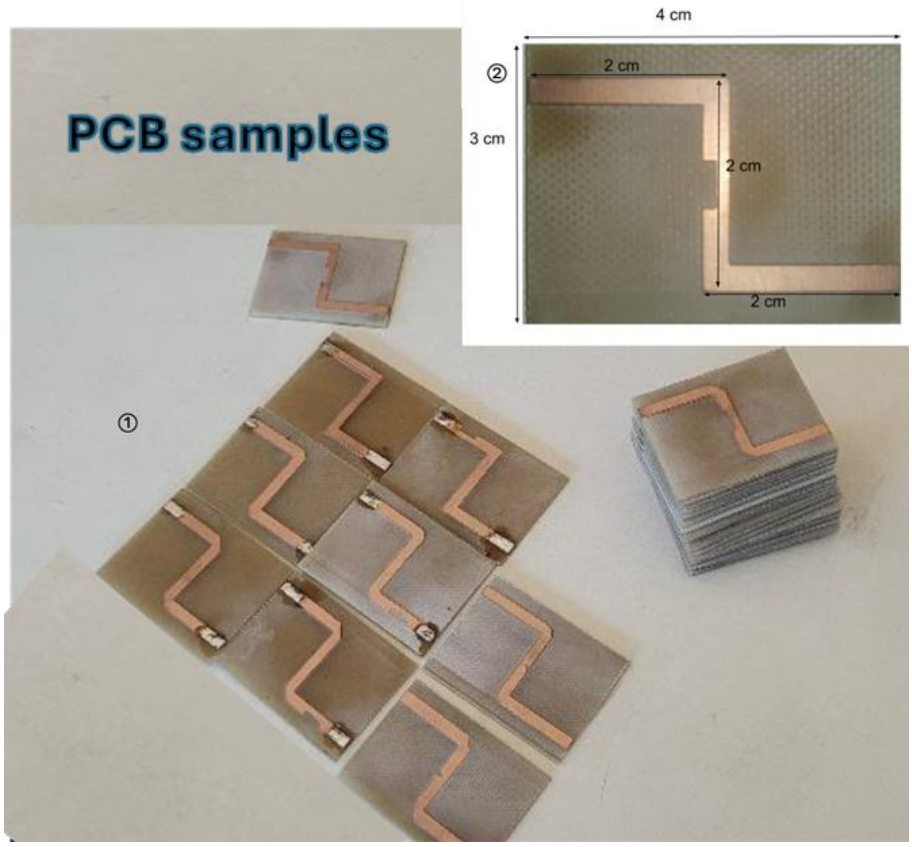

Figure 3: Serie of PCB sample and dimensions

The DUT sample is a PCB measuring 40 mm × 30 mm, on which a 3 mm-wide microstrip line was made using a Technodrill 3 CNC milling machine (see Figure 3-❷). An SMA connector is mounted at each end of the microstrip, the RF generator is connected to one side, while the opposite end is terminated with a short-circuit plug.

3 E-NF test bench operation principle

Figure 4 illustrates the synoptic of the operation principle of the considered E-NF imager test bench. The XY-planar scanner test bench is constituted by a vector signal generator ❶ which generates the input excitation

defined by the amplitude and the operation frequency of the input signal injected to the DUT represented by PCB ❸ and the automatic test bench ❷ controlling the NF probe ❹ scanning motion.

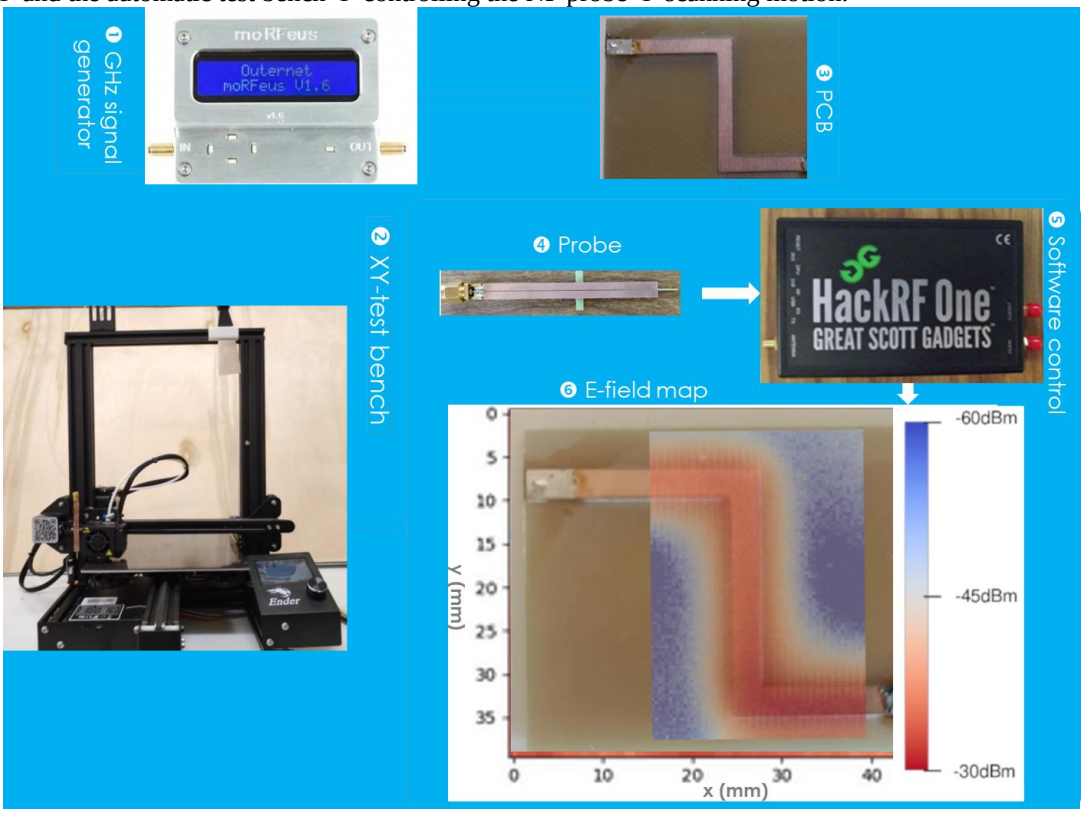

Figure 4: Illustrative diagram of E-NF imager test bench and Sample test with defaults

The measured data are visualized and stored via the software embedding module referenced HackRF One ❺ to generate the E-NF map ❻ in the XY-plan. The core of the system is based on a modified Ender 3 Pro 3D printer. This printer was selected for its ability to perform precise movements (<0.1 mm [10]) while remaining highly affordable (approximately €200). Due to its mechanical design, the printer requires positional referencing before each operation. This homing procedure relies on three micro-switches, one for each axis, to define the origin (zero) position. The second main component of the imaging system is a software-defined radio (SDR), specifically the HackRF One. The SDRs offer substantial advantages over traditional spectrum analyzers, not only because of their significantly lower cost (see [16], e.g., price comparison with Rohde & Schwarz spectrum analyzers), but also due to their ease of use and flexibility in a wide range of RF measurement scenarios [17]. The HackRF One operates from 1 MHz to 6 GHz and connects to a computer via USB, making it a convenient and compact solution for spectral analysis [18]. The third subsystem is a signal generator based on the MoRFeus device. This USB-controlled frequency generator operates across a wide range, from 85 MHz to 5.4

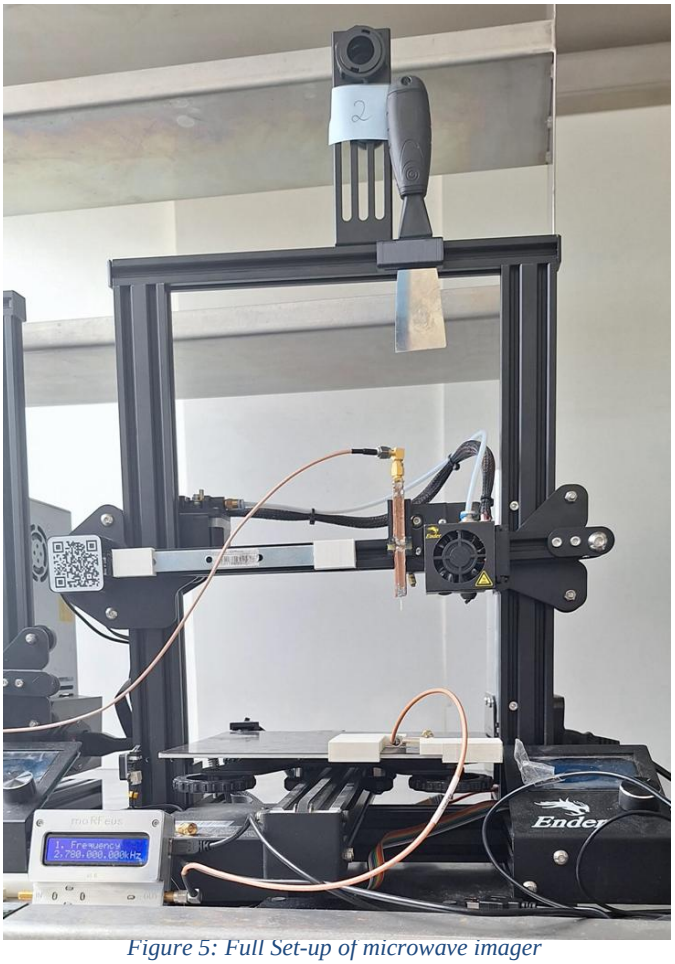

Figure 5: Full Set-up of microwave imager

GHz [19].

It is essential for injecting EM signals into the PCB under test, enabling controlled excitation during the imaging process. The whole system is represented in Figure 5. All components of the imaging system are controlled via a central computer. A dedicated software application was developed specifically for this purpose. This software interfaces with three main elements, such as the 3D printer, the MoRFeus RF signal generator, and the HackRF spectrum analyzer. The 3D printer is operated through a serial interface using a USB-to-serial converter. The control is performed via standard G-code commands, which are widely used across CNC systems [20]. The Python script sends these commands to precisely control probe movement along the two-imaging axes (X and Y). The RF generator is controlled over USB using the Python library provided by the MoRFeus project [21], which allows the user to set frequency and output power programmatically. Finally, the HackRF spectrum analyzer is controlled using the hack RF_sweep command-line utility, which enables signal acquisition by sweeping across a specified frequency range. The sweeping range is centered on the defined frequency and is 2MHz wide. The graphical user interface (GUI) was developed using the Qt framework. It provides an intuitive and centralized control panel that enables the user to operate up to six imaging units simultaneously. Through the interface, the user can configure measurement parameters, including setting the operating frequency for each of the RF signal generators (currently supporting up to four independent sources). In addition to live system control, the GUI also includes features for browsing and displaying previously acquired images stored in the database, enabling quick access to past measurements for comparison or analysis. The control interface representative screenshot is shown in Figure 6.

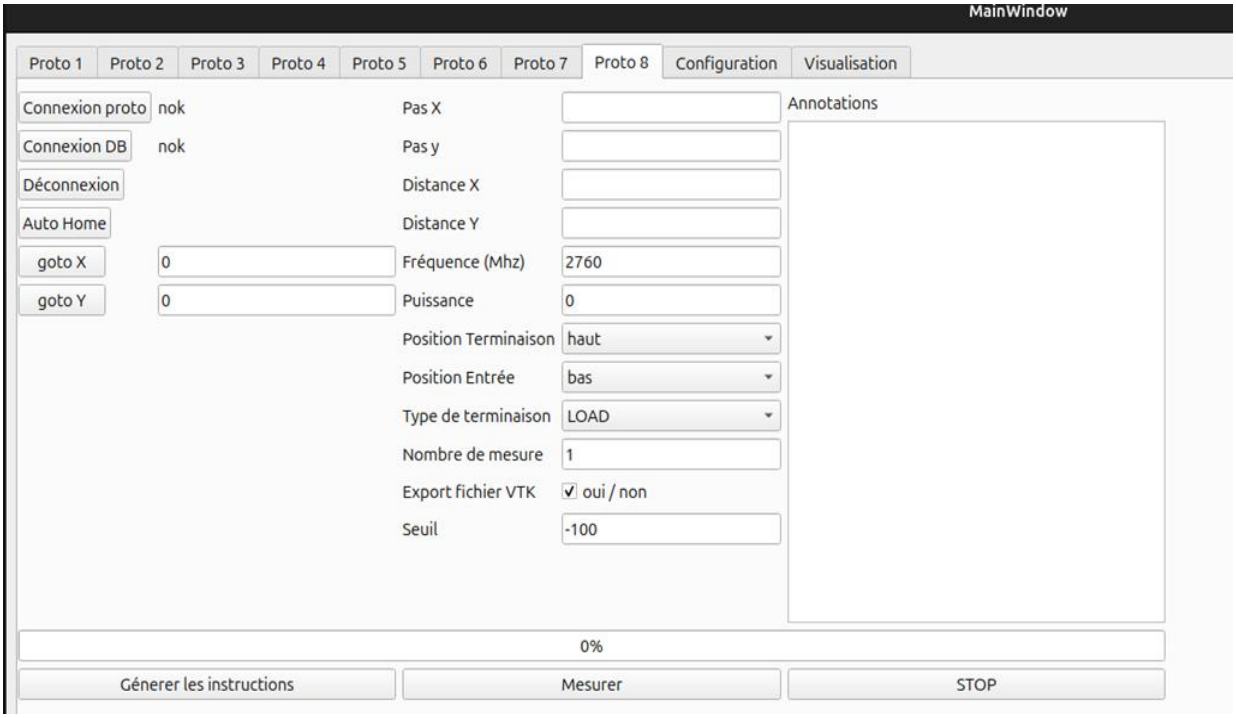

Figure 6: Image of the GUI of the program

Once the user initiates a measurement, a dedicated thread is launched to manage the entire acquisition process. For each measurement point predefined in a separate command file generated in advance, the probe is moved to the corresponding position using G-code instructions. At each point, data is acquired from the HackRF device via the HackRF_sweep command-line utility. The spectral data collected at each position is saved to an individual file. These files are then processed collectively at the end of the scan to reconstruct the final field distribution image. Upon completion of the measurement sequence, all individual data files are read, and the final image is generated and stored in a MongoDB database. This database not only allows for efficient storage and retrieval of measurement results but also supports the visualization and comparison of previous measurements. Additionally, if required, the data can be exported in VTK (Visualization Toolkit) format, enabling further post-processing or visualization with external tools such as ParaView or similar platforms. Additional development was carried out on the software to support its use in a teaching laboratory context. In particular, the application was adapted to run reliably under Windows, and its stability was improved to ensure

consistent operation across multiple imagers working at the same time. For the purposes of practical lab sessions, the configuration of the imager components will be fixed and predefined, significantly reducing the configuration work needed by students. This allows students to focus on the core objectives of the laboratory, namely EM field imaging without being burdened by low-level system configuration tasks.

4 Measuring EM fields: E-NF test result with the developed imager test bench

4.1 Measurement Process and parameters

The scanning procedure is used to acquire the NF image of this PCB. After configuring the imager, the auto-homing sequence is initiated from the graphical user interface. The key parameters include the initial probe position and the distance to the final position, which together define the scanning area as a rectangular region. Additional parameters such as the spatial step size (in both X and Y directions) were set according to the desired resolution. Finally, the RF generator output power is configured to its maximum value (0 dBm) for all subsequent measurements. To validate the performance of the developed imaging system, several EM E-NF measurements were conducted on the previously described PCB sample. These tests aimed to evaluate the system's ability to capture and represent both electric and magnetic field distributions with sufficient spatial resolution and stability. Those tests were also aimed at finding the best measurement height. In the remainder of this document, we will restrict our focus solely to measurements associated with the electrical probe. All the following images are achieved with an open circuit terminating the line.

4.2 Influence of space resolution

The first experiment focused on high-resolution E-NF measurements or mapping over the microstrip structure. Figures 7 present the resulting image acquired using the E-NF probe with a spatial step size of 0.1 mm.

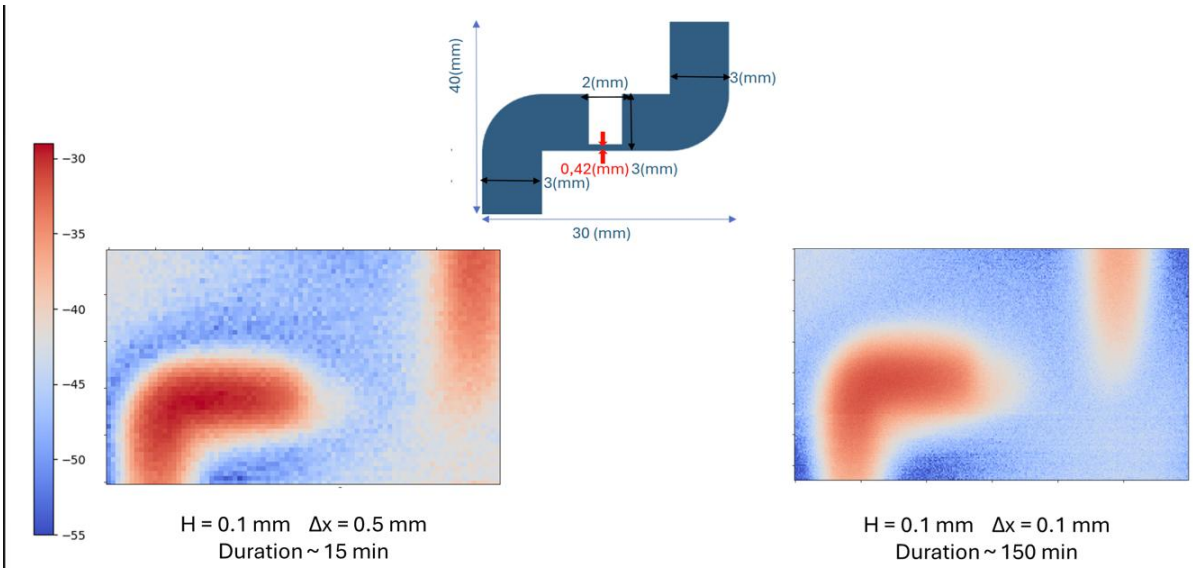

Figure 7: Impact of space resolution of E-NF image and the tested PCB

The measurement was performed at a frequency of 2780 MHz, corresponding to the excitation signal provided by the RF generator. This frequency is right at the peak of the probe resonance curve in the 2 GHz range. We can clearly see on this image the microstrip line with this hole. It is to be noted that the thin copper line running across the hole cannot be seen. The sample selection proposed in Figure 7 is intended to demonstrate the system's measurement capabilities. Specifically, the chosen sample deliberately presents a case of severe line reduction, a feature that remains challenging to detect due to the spatial resolution constraints of current 3-D printing technologies. Overcoming this limitation represents a key objective for the development of next-generation printers.

4.3 Influence of the gap between the DUT PCB sample and probe

The third experiment aimed to assess the impact of the electric field probe's height on image quality. A series of measurements were performed with the probe positioned at varying distances from the microstrip surface, ranging from 0.1 mm to 4.1 mm in 0.5 mm increments. Figure 8 shows the set of resulting images acquired at a frequency of 2780 MHz with a spatial step size of 0.5 mm. These images illustrate how increasing probe height affects both the amplitude and the clarity of the measured electric field distribution. From this experiment, it is

evident that the optimal probe height for such measurements is as close to the surface as possible. The minimal height maximizes sensitivity to the NF variations and minimizes background noise, which otherwise becomes more prominent at greater distances due to reduced field intensity and increased susceptibility to environmental interference.

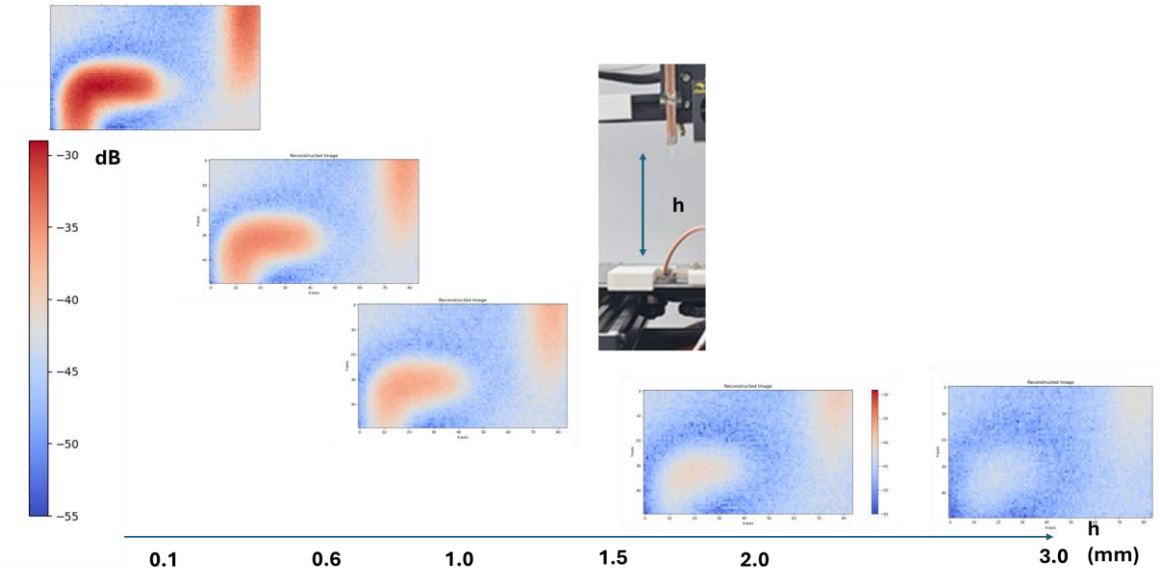

Figure 8 : Influence of the distance E-NF probe to PCB DUT sample

4.4 Influence of the considered test frequency

The performed experiment aimed to assess the impact of the chosen frequency for imaging on the measured E-NF and the subsequent image quality. A series of measurements were performed with the probe positioned at 0.5 mm from the surface and the imaging frequency was increased from 2760 to 2800 MHz with 10 MHz step. The images shown in Figures 9 represent the evolution of the E-NF versus the used frequency close to the resonance. The E-NF mapping is essentially based on the imaging frequency of the used probe resonance range.

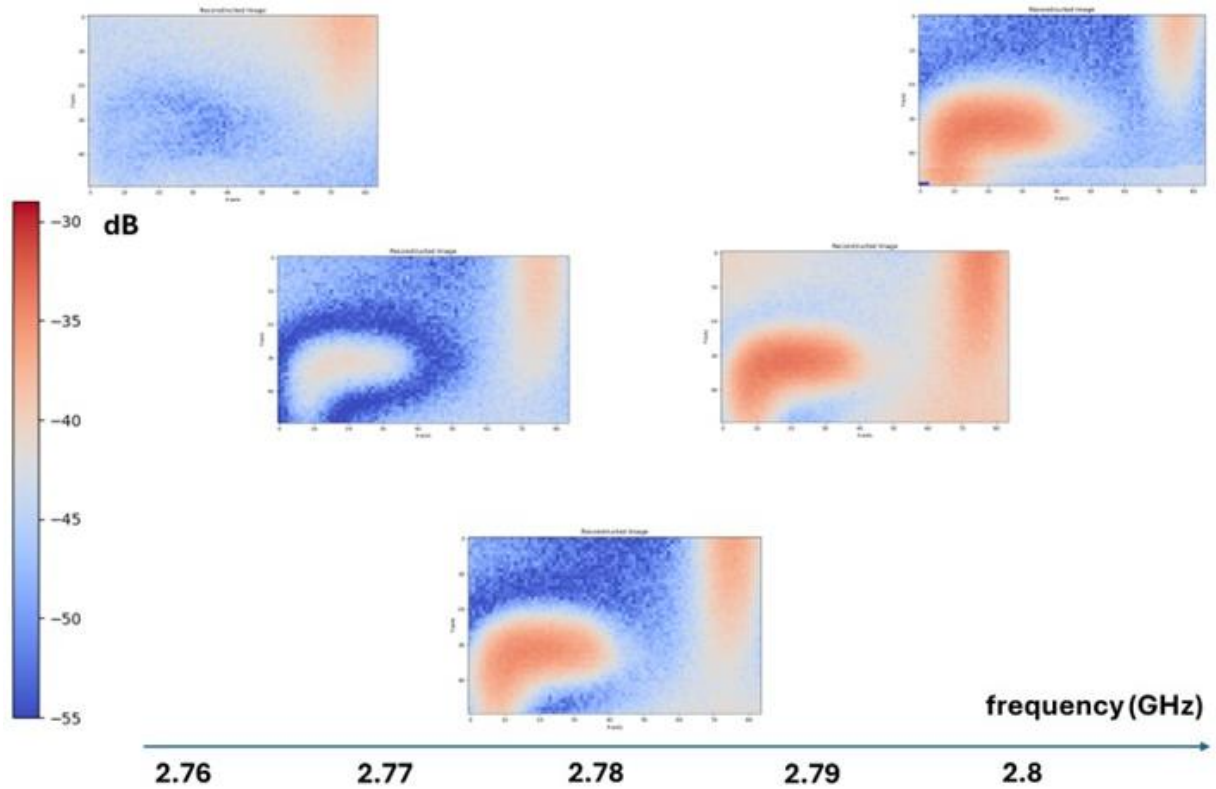

Figure 9 : Evolution of the E-NF image versus the used frequency close to the resonance

5 Conclusion

In this study, we have introduced a low-cost EM field imaging system designed both as a metrological tool and as an educational resource. The device, developed for serial production, is currently deployed in teaching programs at the University of Bourgogne Europe. While the system is subject to the inherent limitations of its class namely, a restricted operational frequency band, limited scanning speed, and the spatial resolution constraints dictated by 3D printing technologies, the methodology adopted is inherently scalable and adaptable. This flexibility opens pathways not only for NF EM measurements but also for susceptibility assessments. In addition, the system's versatility enables the systematic generation of datasets, thus supporting the development and training of deep learning models for future advanced applications.

Références bibliographiques

[1] K. Wiklundh, and P. Stenumgaard, "EMC challenges with 6G," in Proc. 2022 Int. Symp. EMC – EMC Europe, Gothenburg, Sweden, 2022, pp. 19-24.

[2] P. Stenumgaard, "How will 6G affect EMC?", Electronic Environment, https://www.electronic.se/2020/02/25/how-will-6g-affect-emc/

[3] J. Rossignol, D. Stuerga, G. Bailly, A. Harrabi, S. Girard, and S. Lalléchère, "Microwave microscopy applied to EMC problem: Visualisation of electromagnetic field in the vicinity of electronic circuit and effect of nanomaterial coating," Advanced Electromagnetics, vol. 6, no. 2, pp. 33–39, 2017.

[4] P. Maheshwari, V. Khilkevich, D. Pommerenke, H. Kajbaf and J. Min, "Application of emission source microscopy technique to EMI source localization above 5 GHz," 2014 IEEE International Symposium on Electromagnetic Compatibility (EMC), Raleigh, NC, USA, 2014, pp. 7-11.

[5] P. Maheshwari, H. Kajbaf, V. V. Khilkevich and D. Pommerenke, "Emission Source Microscopy Technique for EMI Source Localization," IEEE Trans. EMC, vol. 58, no. 3, pp. 729-737, June 2016.

[6] IEC, "Integrated circuits - Measurement of electromagnetic emissions - Part 1: General conditions and definitions," IEC 61967-1:2018, https://webstore.iec.ch/publication/59799

[7] H. Jia, F. Wan, X. Cheng, V. Mordachev, N. M. Murad and B. Ravelo, "Electric near-field scanning for electronic PCB electromagnetic radiation measurement", Measurement, Vol. 228, No. 114355, Feb. 2024, pp. 1-8.

[8] M. Kanda, "Standard probes for electromagnetic field measurements," IEEE Trans. AP, vol. 41, no. 10, 1993, pp. 1349-1364.

[9] X. Peng, et al., "Simulation-based electromagnetic radiation anti-interference measures and verification," Journal of Microwaves, vol. 30, no, S2, 2014, pp. 58-60.

[10] N. Mai-Khanh, et al, "An Integrated High-Precision Probe System in 0.18-µm CMOS for Near-Field Magnetic Measurements on Cryptographic LSIs," IEEE Sensors, vol. 13, no. 7, 2013, pp. 2675-2682.

[11] https://yictechnologies.com/emc-desktop-scanner/, Accessed Apr. 20, 2025.

[12] Y. Liu, et al., "Time-Domain Magnetic Dipole Model of PCB Near-Field Emission," IEEE Trans. EMC, vol. 58, no. 5, Oct. 2016, pp. 1561-1569.

[13] Y. Liu and B. Ravelo, "Fully time-domain scanning of EM near-field radiated by RF circuits," PIER B, vol. 57, 2014, pp. 21-46.

[14] A. Roy, "Imagerie Microondes : Reflet de CEM en 5G (In French)", Master Thesis, University of Bourgogne Europe, 2024.

[15] https://www.changpuak.ch/electronics/MagneticFieldProbe.php, Accessed Apr. 20, 2025.

[16] https://theemcshop.com/manufacturers/rohde-schwarz-rf-test-equipment/rohde-schwarz-spectrum-analyzers/?srsltid=AfmBOoroYFc78QoVrd0LrYhj40zdz8oIT6U2EDFrwrjI4ahU9yb0t1FX, Accessed Apr. 20, 2025.

[17] https://www.scielo.br/j/jmoea/a/TCg4wdgNMmHZVK9TGZKZS8C/?lang=en, Accessed Apr. 20, 2025.

[18] https://hackrf.readthedocs.io/en/latest/hackrf_one.html, Accessed Apr. 20, 2025.

[19] https://www.crowdsupply.com/othernet/morfeus, Accessed Apr. 20, 2025.

[20] https://www.science.smith.edu/resources/cdf/pdf_files/Techno_GCODE%20Commands.pdf, Accessed Apr. 20, 2025.

[21] https://pypi.org/project/morfeus/, Accessed Apr. 20, 2025.